Controllable nonlinear refraction characteristics in hydrogenated nanocrystalline silicon

D. Q. Zheng,[1] W. A. Su,[2] Q. H. Ye,[1] and W. Z. Shen[1,a)]
[1]*Laboratory of Condensed Matter Spectroscopy and Opto-Electronic Physics, and Key Laboratory of Artificial Structures and Quantum Control (Ministry of Education), Department of Physics and Astronomy, and Institute of Solar Energy, Shanghai Jiao Tong University, 800 Dong Chuan Road, Shanghai 200240, China*
[2]*Faculty of Science, Jiangxi University of Science and Technology, 86 Hong Qi Road, Ganzhou, Jiangxi 341000, China*

(Received 21 January 2014; accepted 22 January 2014; published online 4 February 2014)

Nonlinear refraction (NLR) of hydrogenated nanocrystalline silicon (nc-Si:H) has been investigated through the close aperture *Z*-scan method. We demonstrate a significant NLR and a unique feature of controllable NLR characteristics between saturable and Kerr NLR with the incident photon energy. We numerically evaluate the proportion of these two mechanisms in different wavelengths by a modified NLR equation. The band tail of nc-Si:H appears to play a crucial role in such NLR responses. © *2014 AIP Publishing LLC*.
[http://dx.doi.org/10.1063/1.4864132]

Nonlinear optical devices are gaining an increasing importance, thanks to their faster response, wider bandwidths, less transmission loss, etc., compared with electronic devices. A great number of studies focusing on the nonlinear optical devices[1–5] have been conducted over the past decades, among which most are still in the research stage though. Past researches mostly focus on the organic[1,2] or multiple-component materials,[3–5] which either have too short usable life or too complex and expensive to allow mass production. Furthermore, the nonlinear property of the conventional material, which is always limited to one particular type, i.e., saturable nonlinear refraction (SNLR),[6,7] reverse saturable nonlinear refraction (RSNLR),[8] or Kerr nonlinear refraction (KNLR),[9,10] or other nonlinear refraction (NLR) mechanisms, heavily restricts its application. In order to promote the use of nonlinear optical devices, we need to not only reduce the material cost but also develop the material with tunable NLR behavior for wider applications.

Here, we present the highly sensitive transition of NLR mechanisms between SNLR and KNLR in the cheap material of hydrogenated nanocrystalline silicon (nc-Si:H) thin film. As an interesting semiconductor, nc-Si:H exhibits great advantages benefiting from its compatibility with the current semiconductor manufacturing process. Since it can be grown by plasma-enhanced chemical vapor deposition (PECVD) at low temperature and on large area, nc-Si:H is easily to be integrated with most devices.[11,12] Through the detailed investigation of the NLR of nc-Si:H by close aperture (CA) *Z*-scan measurements,[13] we have observed a unique feature of transition between SNLR and KNLR with incident photon energy slightly less than the bandgap of the sample. We attribute this controllable NLR behavior of nc-Si:H to band tail states and quantify the contribution of these two NLR mechanisms at different wavelengths by a modified NLR equation. This significant finding breaks the restriction of the particular one nonlinear refraction mechanism in the traditional materials and devices, and will have a great potential to boost nonlinear refraction applications.

The nc-Si:H thin films were grown on glass substrates by PECVD system. Detailed growth conditions can be readily found in our previous works.[14,15] The physical characterizations were measured with x-ray diffraction and high-resolution transmission electron microscopy (nanocrystalline size *d*), Raman spectroscopy (crystalline volume fraction X_c), optical transmission measuremen(d ele20TDv0.3(J0-1253.TD[(fi11.(rosc)
lo0-1253ed Ti:TD4(a)10.5(p)0(p)13.5(h)0(i)15.6(r)0(e)-229.2(l)0(a)13.7(s
SNLR
using the CA *Z*-scan, nc-Si:H exhibits great met th15.6(e)-267.3(co)11253ndition11.(r-6.7974-1.2019TD[(of)-227.2(th)15.(
$_{00}$ spatial mode, 100 fs
duration, 82 MHz repetion rate, and tunable wavelength]TJ0-1.2019T
[17]
which is two orders of magnitudes smaller than the size of bem waist. So we can onsider that the carriers are trapped in where they are ge-1253.rated.

The pure NLR *Z*

20 mm, and the y-axis in the CA/OA *Z*-scan curves represents the transmittance normalized to that at $z = 0$ mm (the beam waist point). The experiments were also performed on the pure glass substrate and no significant contribution from the substrate was found.

Fig. 1(a) shows the λ-dependent CA/OA *Z*-scan transmittance spectra of the sample at $I_0 = 0.36\,\mathrm{GW/cm^2}$, where I_0 is the irradiance of incident laser pulses at focus (i.e., $z = 0$) excluding the Fresnel reflection loss.[13] We can find that all the spectra display the valley-peak pattern, indicating a positive NLR index (i.e., self-focusing), which is consistent with other experiments on silicon nanostructures.[19,20] However, as the photon energy of the incident irradiance slightly changes from 1.49 to 1.55 eV (i.e., λ from 830 to 800 nm), the difference between the normalized peak (T_p) and valley (T_v) transmittance $\Delta T_{p\text{-}v}$ ($=T_p - T_v$) exhibits a significant reduction from 0.13 to 0.03. In order to reveal the physical nature of the high sensitivity of the nonlinear behavior to the incident wavelength, we present in Fig. 1(b) I_0-dependent *Z*-scan curves at two typical λ of 830 and 800 nm. Interestingly, different NLR behaviors have clearly been observed. At a long $\lambda = 830$ nm, $\Delta T_{p\text{-}v}$ remains almost unchanged as I_0 varies from 1.41 to 0.24 GW/cm^2. In contrast, at a short $\lambda = 800$ nm, $\Delta T_{p\text{-}v}$ decreases significantly with the incident intensity, showing a strong I_0 dependence, which is totally different from that at $\lambda = 830$ nm.

These unique NLR behaviors of our sample can be interpreted by means of the influences of SNLR and KNLR. Detailed physics picture can be found in Fig. 2(a). Since the incident photon energy ranging from 1.49 to 1.55 eV (i.e., λ varies from 830 to 800 nm) is slightly less than the bandgap of the nc-Si ($E_g = 1.56$ eV), the excited electrons upon the

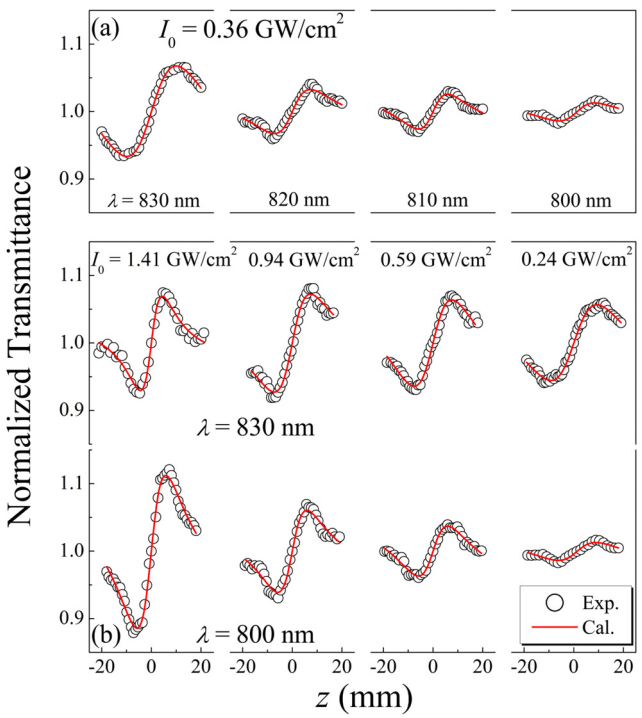

FIG. 1. Measured and calculated (a) λ-dependent CA/OA *Z*-scan curves at $I_0 = 0.36\,\mathrm{GW/cm^2}$ and (b) I_0-dependent CA/OA *Z*-scan curves at $\lambda = 830$ nm and 800 nm.

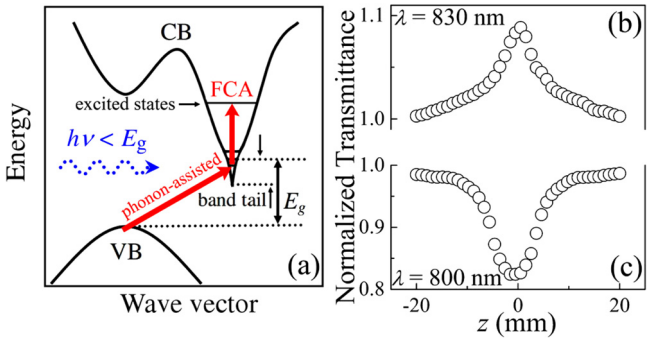

FIG. 2. (a) Schematic bandgap diagram showing feasible NLR mechanisms. (b) and (c) OA *Z*-scan curves at $\lambda = 830$ and 800 nm, respectively.

below-bandgap incident irradiance may transit from the valence band to the exponential band tail with a width of tens of meV[21,22] through a phonon-assisted one-photon absorption process. For the long λ (i.e., 830 nm), the excited electrons can just get to the bottom of the band tail, which indicates that it is easy to reach the absorption saturation due to the low density of states there, leading to the saturation of the carrier density. This saturable absorption has been confirmed by the observed peak pattern of the OA *Z*-scan curve (at $\lambda = 830$ nm and $I_0 = 1.67\,\mathrm{GW/cm^2}$) in Fig. 2(b). Since silicon has the significant carrier dispersion effect,[23] which relates the variation in the density of carriers to the changes in the refraction index, the NLR saturation (i.e., the SNLR) arises.

When the energy of the incident irradiance increases to be very close to the bandgap (i.e., for a short $\lambda = 800$ nm), it needs much higher incident intensity to reach that absorption saturation owning to the increased density of the band tail states. At the same time, the one-photon induced free carrier absorption (FCA) begins to emerge since more electrons are allowed in the conduction band tail. Subsequently, the absorption coefficient increases with the incident irradiance density, which can be evidenced through the valley pattern of OA *Z*-scan curve in Fig. 2(c) (at $\lambda = 800$ nm and $I_0 = 1.67\,\mathrm{GW/cm^2}$). The refraction index demonstrates an increment with the incident irradiance via carrier dispersion (i.e., the KNLR).

From the discussion above, we can come to the conclusion that the λ-driven SNLR and KNLR both exist in the wavelength range of 830–800 nm. The SNLR appears to be the main NLR behavior in long λ, while the KNLR gradually begins to dominate the processes in short λ. To further quantify the contribution of the SNLR and KNLR in different λ, we dive into the data of Fig. 1. As we know, the normalized transmittance $T(z)$ of typical CA (finite aperture at the far field) *Z*-scan is given by[13]

$$T(z) = 1 + \frac{4x\Delta\phi}{(x^2+9)(x^2+1)}, \tag{1}$$

where $x = z/z_0$ with $z_0 = \pi\omega_0^2/\lambda$ the Rayleigh range of the lens (ω_0 the beam waist), and $\Delta\phi = kn_{\mathrm{total}}I_0L_{\mathrm{eff}}$ is the nonlinear phase change with $k = 2\pi/\lambda$ the wave vector, n_{total} the NLR index defined as $n = n_0 + n_{\mathrm{total}}I$ (n the whole refraction, including both linear and nonlinear contributions, n_0 the

linear refraction and I the beam irradiance), and $L_{\text{eff}} = (1 - \exp(-\alpha_0 L))/\alpha_0$ the effective sample length. As clearly seen in Fig. 1, the calculated transmittance (red curves) excellently fits the experimental Z-scan results (black open circles), where we can obtain n_{total} from the best fits.

The yielded I_0-dependent n_{total} at various λ are presented as open circles in Figs. 3(a)–3(d). On one hand, we can see that the magnitude of n_{total} achieves 10^{-2}–10^{-1} cm^2/GW, which is several orders of magnitudes larger than the conventional nonlinear material, such as $LiNbO_3$ (Ref. 24) and $BaMgF_4$ (Ref. 25). On the other hand, n_{total} shows different I_0-dependent behavior at different λ. At $\lambda = 830$ nm (Fig. 3(a)), n_{total} decreases rapidly from 0.22 to 0.05 cm^2/GW as the incident intensity increases. As λ gets shorter, the diminution of n_{total} becomes slower (Figs. 3(b) and 3(c)). When λ decreases to 800 nm, n_{total} keeps a consistent ~0.07 over various I_0 (Fig. 3(d)).

A simple model based on the carrier dispersion effect is presented to quantify the interesting n_{total} behavior and numerically evaluate the proportion of SNLR and KNLR. Taking the contribution of the carriers in each energy level into account, the refraction index n of the sample can be expressed as[26]

$$n = 1 + \sum \eta N, \tag{2}$$

where the constant 1 is the refraction index of vacuum, η and N are the refraction volume and the carrier density of each energy level. For SNLR, the electrons transfer from valence band to the band tail through one-photon absorption process. N of the valence band (N_{VB}) and the band tail (N_{BT}) can be solved through the rate equation[26]

$$\begin{cases} \dfrac{\partial N_{\text{BT}}}{\partial t} = \dfrac{\alpha I}{h\nu} - \dfrac{N_{\text{BT}}}{\tau_1} \\ N_{\text{W}} = N_{\text{BT}} + N_{\text{VB}}, \end{cases} \tag{3}$$

where $\alpha = \alpha_0/(1 + I/I_{\text{S}})$ is the absorption efficient[14] with I_{S} the saturation irradiance, $h\upsilon$ the photon energy, τ_1 the recombination lifetime from band tail to valence band, and N_{W} the carrier density of the whole system. Therefore, we can obtain n of the sample at a steady state as

$$n = n_0 + \frac{\alpha_0 \tau_1 (\eta_{\text{BT}} - \eta_{\text{VB}})}{h\nu} \frac{I}{1 + I/I_{\text{S}}} = n_0 + n_{\text{SR}} \frac{I}{1 + I/I_{\text{S}}}, \tag{4}$$

where η_{VB} and η_{BT} are the refraction volume of valence band and conduction band tail, respectively, $n_0 = 1 + \eta_{\text{VB}} N_{\text{W}}$ the linear refraction index when all the electrons are in the valence band, and $n_{\text{SR}} = \alpha_0 \tau_1 (\eta_{\text{BT}} - \eta_{\text{VB}})/h\upsilon$ the saturable NLR index.

While for KNLR, the electrons can further transfer from the band tail to the excited states in the conduction band through FCA. Only consider the contribution of the carriers in the band tail and excited states, N_{BT} and N of the excited states (N_{ES}) can be solved by[26]

$$\begin{cases} \dfrac{\partial N_{\text{ES}}}{\partial t} = \dfrac{\sigma_{\text{BT}}}{h\nu} I N_{\text{BT}} - \dfrac{N_{\text{ES}}}{\tau_2} \\ N'_{\text{W}} = N_{\text{BT}} + N_{\text{ES}}, \end{cases} \tag{5}$$

where σ_{BT} is the absorption cross section of conduction band tail, τ_2 the recombination lifetime from excited states to band tail, and N'_{W} the sum carrier density of band tail and excited states. With $h\nu/\sigma_{\text{BT}}\tau_2 \gg I$, we can get n at a steady state as follows:

$$n \approx n'_0 + (\eta_{\text{ES}} - \eta_{\text{BT}}) \frac{\sigma_{\text{BT}} \tau_2 N'_{\text{W}}}{h\nu} I = n'_0 + n_{\text{KR}} I \tag{6}$$

with $n_{\text{KR}} = (\eta_{\text{ES}} - \eta_{\text{BT}})\sigma_{\text{BT}}\tau_2 N'_{\text{W}}/h\upsilon$ the Kerr NLR index, η_{ES} the refraction volume of excited states, and $n'_0 = 1 + \eta_{\text{BT}} N'_{\text{W}}$ the refraction index without FCA.

Taking these two NLR contributions together, we can get n_{total} expressed as follows:

$$n_{\text{total}}(I) = \frac{n_{\text{SR}}}{1 + I/I_{\text{S}}} + n_{\text{KR}}, \tag{7}$$

where the NLR index consists of the SNLR term $n_{\text{SR}}/(1 + I/I_{\text{S}})$ and the KNLR term n_{KR}. The value of n_{SR} is ~0.69 cm^2/GW calculated from the best fits in Figs. 3(a)–3(d) (red curves). I_{S} and n_{KR} are sensitive to λ and dominate the SNLR to KNLR switching. The λ-dependent I_{S} and n_{KR} are presented in Figs. 3(e) and 3(f). At $\lambda = 830$ nm, I_{S} is 0.11 GW/cm^2 and n_{KR} is nearly 0, indicating a nearly pure SNLR. As λ decreases, both I_{S} and $|n_{\text{KR}}|$ overall increase, implying that SNLR becomes weakened, while KNLR gets enhanced. Finally, at $\lambda = 800$ nm, I_{S} is ~500 GW/cm^2 ($\gg I_0$) and n_{KR} is −0.62 cm^2/GW, indicating a nearly pure KNLR.

As a consequence of the significant NLR and highly sensitive λ-driven SNLR to KNLR switching, nc-Si:H shows great potential in the nonlinear photonic applications. Firstly, we can take advantage of either SNLR or KNLR of nc-Si:H individually to realize the corresponding devices. Secondly, we may combine these two NLR mechanisms to achieve application, such as the adjustable device, which can be modulated between step-type (at $I = 0$ for "0" and at $I > I_{\text{S}}$ for "1" realized by SNLR) and gradient-type (refraction index gradient changes with incident irradiance realized by

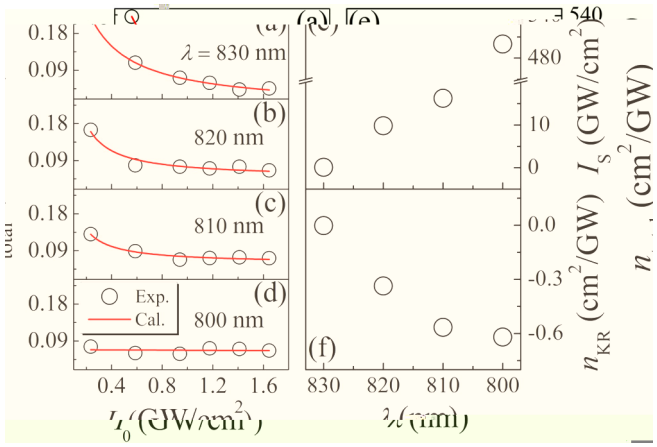

FIG. 3. (a)–(d) I_0-dependent nonlinear refraction index n_{total} at various incident wavelengths. Both experimental data (open circles) and best fit (red curves) are shown. (e) and (f) λ-dependent I_{S} and n_{KR}.

KNLR) by the incident wavelength for different requirements. Moreover, as the bandgap of nc-Si:H can be easily tuned during the growth process, and an increase in bandgap at a fixed λ is effectively the same as a decrease in λ at a fixed bandgap, we may fabricate the construction with the gradient or periodic bandgap to realize gradient or periodic refraction index for waveguide, photonic crystal, and many other applications.

In summary, we have used the CA *Z*-scan technique to observe NLR responses of nc-Si:H greatly tunable with the incident wavelength. We demonstrate the significant NLR and highly sensitive λ-driven SNLR to KNLR switching in this cheap material. These NLR responses have turned out to be well-described by the modified NLR equation, suggesting that the NLR mechanism of nc-Si:H may rely on its band tail states. The present work proves the feasibility of the application of nc-Si:H to various nonlinear optical devices via the sensitive controllable NLR behavior.

This work was supported by National Major Basic Research Project (2012CB934302) and Natural Science Foundation of China (11174202 and 61234005).

[1]S. A. Haque and J. Nelson, Science **327**, 1466 (2010).
[2]J. Clark and G. Lanzani, Nat. Photonics **4**, 438 (2010).
[3]R. Schiek, A. Solntsev, and D. Neshev, Appl. Phys. Lett. **100**, 111117 (2012).
[4]F. Setzpfandt, M. Falkner, T. Pertsch, W. Sohler, and R. Schiek, Appl. Phys. Lett. **102**, 081104 (2013).
[5]P. C. Ray, Chem. Rev. **110**, 5332 (2010).
[6]T. Catunda and L. Cury, J. Opt. Soc. Am. B **7**, 1445 (1990).
[7]L. Demenicis, A. Gomes, D. Petrov, C. B. de Araújo, C. P. de Melo, C. G. Dos Santos, and R. Souto Maior, J. Opt. Soc. Am. B **14**, 609 (1997).
[8]C. F. Li, Y. X. Wang, and X. R. Zhang, Chin. Phys. **9**, 194 (2000).
[9]M. Bache and F. W. Wise, Phys. Rev. A **81**, 053815 (2010).
[10]C. Wang, Y. Fu, Z. Zhou, Y. Cheng, and Z. Xu, Appl. Phys. Lett. **90**, 181119 (2007).
[11]A. Martínez, J. Blasco, P. Sanchis, J. V. Galán, J. García Rupérez, E. Jordana, P. Gautier, Y. Lebour, S. Hernández, and R. Spano, Nano Lett. **10**, 1506 (2010).
[12]K. Narayanan and S. F. Preble, Opt. Express **18**, 8998 (2010).
[13]M. Sheik-Bahae, A. Said, T. Wei, D. Hagan, and E. Van Stryland, IEEE J. Quantum Electron. **26**, 760 (1990).
[14]Y. J. Ma, J. I. Oh, D. Q. Zheng, W. A. Su, and W. Z. Shen, Opt. Lett. **36**, 3431 (2011).
[15]D. Q. Zheng, Y. J. Ma, L. Xu, W. A. Su, Q. H. Ye, J. I. Oh, and W. Z. Shen, Opt. Lett. **37**, 3639 (2012).
[16]*Handbook of Optical Constants of Solids*, edited by E. D. Palik (Academic, 1985).
[17]V. Svrcek, I. Pelant, J. Kocka, B. Rezek, A. Fejfar, A. Poruba, and J. Tousek, J. Appl. Phys. **89**, 1800 (2001).
[18]A. Said, M. Sheik-Bahae, D. J. Hagan, T. Wei, J. Wang, J. Young, and E. V. Stryland, J. Opt. Soc. Am. B **9**, 405 (1992).
[19]G. V. Prakash, M. Cazzanelli, Z. Gaburro, L. Pavesi, F. Iacona, G. Franzo, and F. Priolo, J. Appl. Phys. **91**, 4607 (2002).
[20]S. Hernández, P. Pellegrino, A. Martínez, Y. Lebour, B. Garrido, R. Spano, M. Cazzanelli, N. Daldosso, L. Pavesi, and E. Jordana, J. Appl. Phys. **103**, 064309 (2008).
[21]L. Chen, J. Tauc, and Z. Vardeny, Phys. Rev. B **39**, 5121 (1989).
[22]A. F. Halverson, J. J. Gutierrez, J. D. Cohen, B. Yan, J. Yang, and S. Guha, Appl. Phys. Lett. **88**, 071920 (2006).
[23]R. Soref and B. Bennett, IEEE J. Quantum Electron. **23**, 123 (1987).
[24]J. Burghoff, H. Hartung, S. Nolte, and A. Tünnermann, Appl. Phys. A **86**, 165 (2007).
[25]J. J. Chen, X. F. Chen, A. H. Wu, H. J. Li, Y. L. Zheng, Y. Z. Ma, L. W. Jiang, and J. Xu, Appl. Phys. Lett. **98**, 191102 (2011).
[26]C. Li and Y. Wang, Proc. SPIE **3467**, 241 (1998).